Trabajos de Geología, Universidad de Oviedo, 30 : 87-95 (2010)

Oviedo (Spain) 1-3 July 2008 International Meeting of Young Researchers in Structural Geology and Tectonics
YORSGET

Kinematic approach by means of AMS study in the Boltaña anticline (southern Pyrenees)

T. MOCHALES[1*], E. L. PUEYO[1], A. M. CASAS[2] AND A. BARNOLAS[3]

[1]*IGME, Oficina de Proyectos de Zaragoza. c/ Manuel Lasala 44, 50006 Zaragoza, Spain.*

[2]*Departamento de Ciencias de la Tierra, Universidad de Zaragoza. c/ Pedro Cerbuna 12, 50009 Zaragoza, Spain.*

[3]*Instituto Geológico y Minero de España, c/ Río Rosas 23, 28003 Madrid, Spain*

[*]*e-mail: tania@igme.es*

Abstract: In this work we present AMS results obtained from several profiles in the Lutetian, carbonate-slope sequence located in the eastern limb of the Boltaña anticline. The AMS analyses allow us to define the deformational events related to the formation of the Boltaña anticline and its progressive rotation during Eocene (Late Lutetian) times, acting as a passive marker of the deformation, after a very early record of LPS during diagenesis.

Keywords: anisotropy of magnetic susceptibility, weak deformation, Boltaña anticline, Ainsa basin, Southern Pyrenees.

The study of the anisotropy of magnetic susceptibility (AMS) is a useful tool for the analysis of deformation in weakly deformed rocks (Parés *et al.*, 1999 and references therein). In sedimentary rocks, AMS can indicate tectonic fabrics modifying the initial, sedimentary fabric (i.e. K3 perpendicular to bedding), thus helping in the unravelling of the deformational history of sedimentary basins (Soto *et al.*, 2003, 2007). The main indicator for tectonic deformation is the magnetic lineation, defined by the orientation of K1 (long axis of the magnetic susceptibility ellipsoid). When AMS carriers are paramagnetic minerals (mainly phylosillicates) a direct relationship can be established between the orientation of magnetic susceptibility axes and mineral orientation (Rochette, 1987; Martín-Hernández and Hirt, 2003).

The Boltaña anticline, located in the eastern sector of the Jaca-Pamplona Basin, is a key area to help understanding the South Pyrenean Central Unit evolution. The interest of this structure lies mainly in its orientation (N-S), oblique to the main Pyrenean structural trend (WNW-ESE), as it occurs with other structures from the western part of the southern Pyrenees, and the syn-tectonic sedimentary record in its limbs. The N-S orientation of the Boltaña and Mediano anticlines (Fig. 1) contrasts with the orientation of frontal structures, both the Marginal Sierras and External Sierras, and the overall structure of the Pyrenean range, characterised by a system of folds and thrusts in a WNW-ESE trend.

The present paper deals with the problem of geometry and kinematics of these oblique structures, specifically the Boltaña anticline, by means of AMS analysis. The results obtained from weakly deformed marlstones allow us to define the deformation events related to the formation of the Boltaña anticline and its progressive rotation during Eocene (Late Lutetian) times.

Geological setting

The Boltaña anticline is located in the southern central Pyrenees (Figs. 1 and 2), in the western termina-

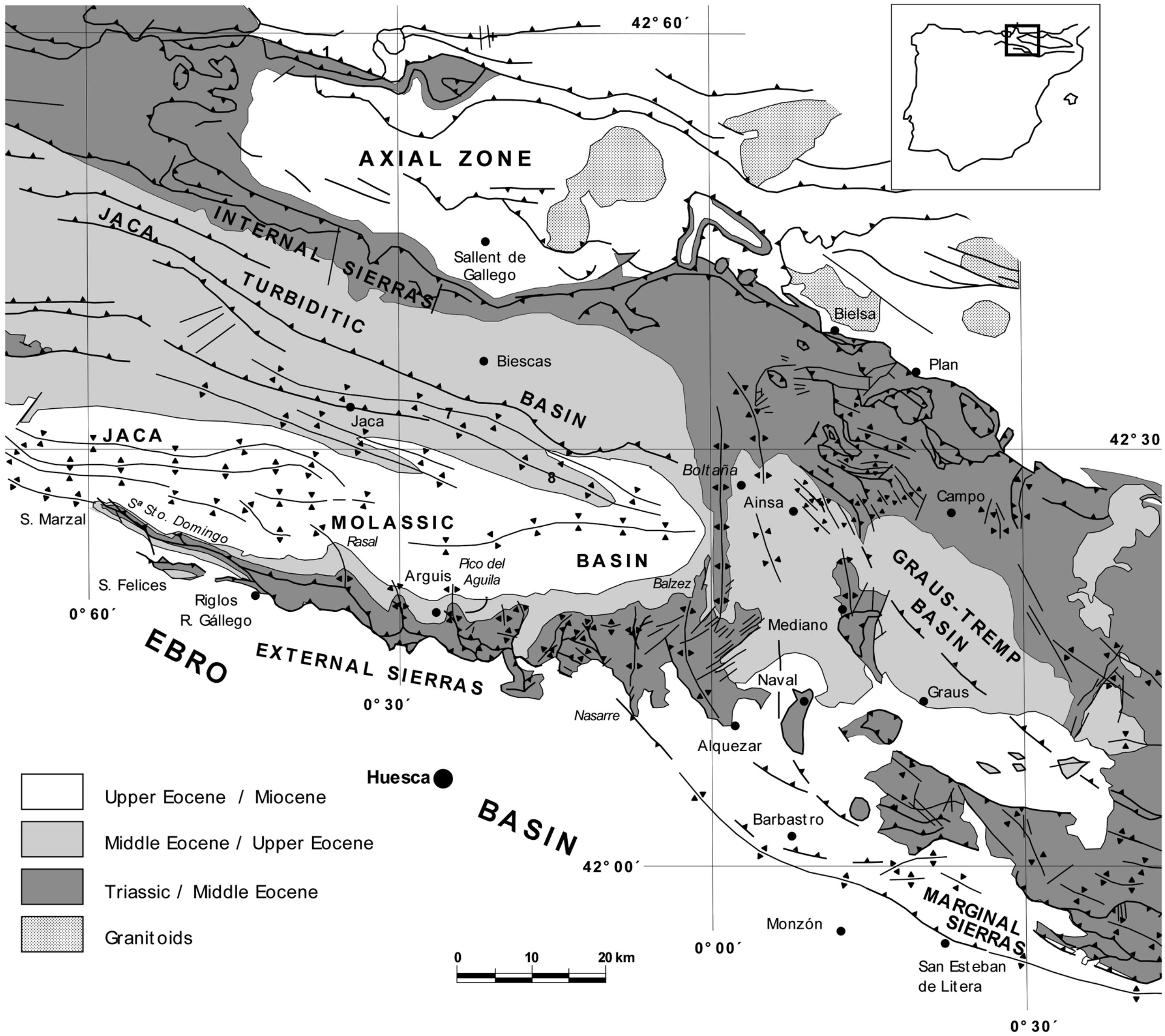

Figure 1. Geological map of the External Sierras within the structural frame of the South-Central Pyrenees, modified from Pueyo *et al.* (1999). In the figure we can distinguish the Jaca Basin on the west side and the Graus-tremp Basin on the east side of the Boltaña anticline which split them up. Also, we see the location of the Marginal, External and Internal Sierras and several anticlines pointed out in the text.

tion of the South Pyrenean Central Unit (SPCU). It defines an area of N-S trending folds (Mediano anticline, Buil syncline, Boltaña anticline), linking the E-W trending structures of the SPCU with the Aragonese External Sierras, where N-S folds (Balzez, Pico del Águila, Bentue de Rasal, Rasal) (Fig. 1) are not so continuous along the trend.

The Boltaña anticline is linked to an underlying non-outcropping thrust that defines the westward vergence of the fold (Cámara and Klimowitz, 1985; Soto and Casas, 2001). The thrust-anticline system is décolled on the Triassic evaporites that form the detachment level to the south Pyrenean thrust system. Pre-tectonic folded cover rocks above the evaporitic detachment are mainly of Upper Cretaceous and Paleogene age.

The shallow Lutetian carbonate platform corresponds to the Guara Fm (Puigdefábregas, 1975) in the sense of Barnolas *et al.* (1991). The lower part of the carbonate slope facies, mostly represented by marls and nodular marly limestones, belongs to Las Paules Fm (De Federico, 1981). It is equivalent to the progradational carbonate platform margin that ends in the Coscollar carbonate platform wedge. Marls with abundant carbonate debris sheet layers represent the upper part of the carbonate slope facies (La Patra Fm,

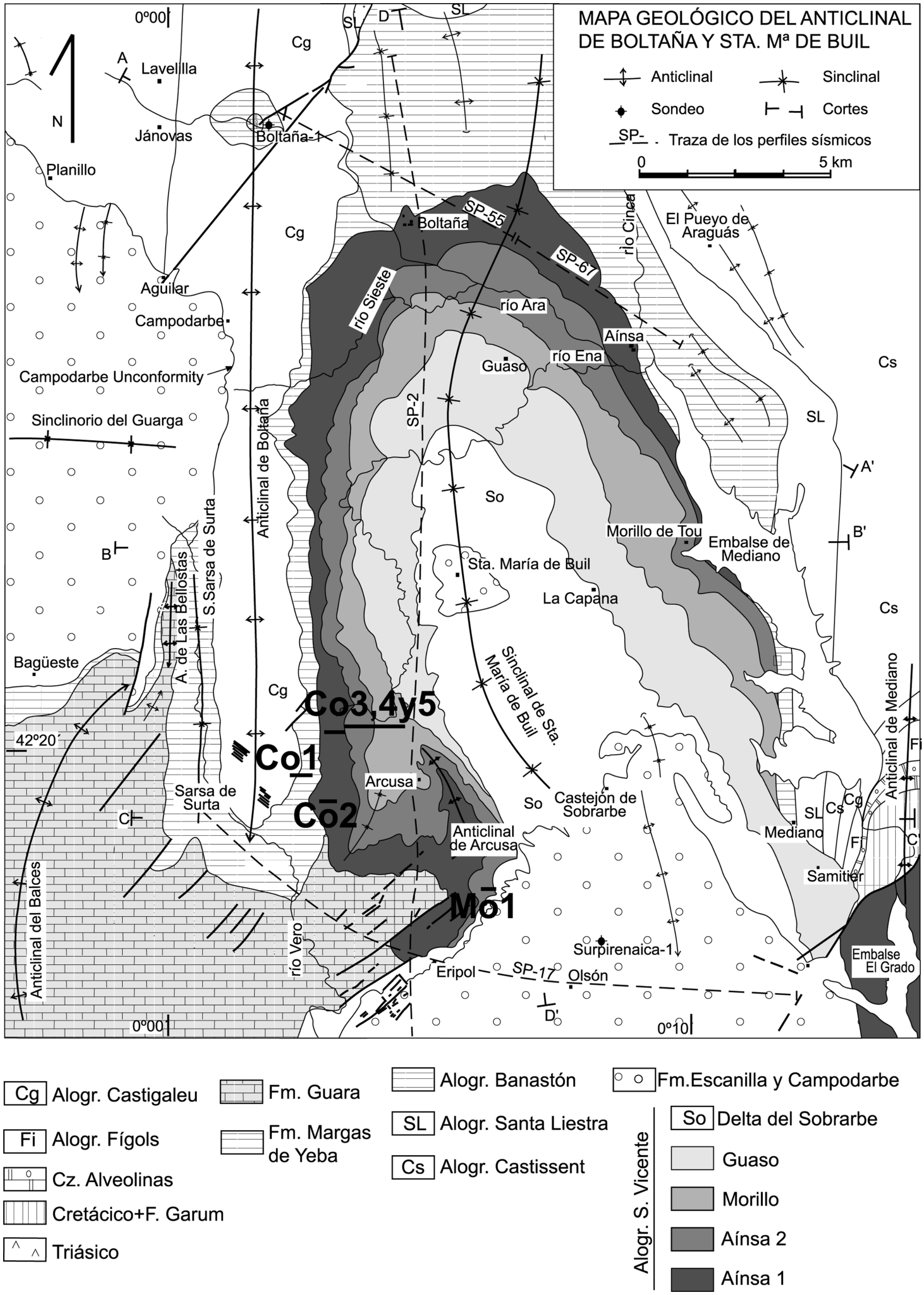

Figure 2. Geological sketch map of the Boltaña and Mediano anticlines (modified from Soto and Casas, 2001). From the sections underlined in black were extracted the samples used in this study.

De Federico, 1981). The lower part of Las Paules Fm is assimilated in the Banastón Allogroup whereas La Patra Fm is equivalent to the Ainsa 1 sequence of the San Vicente Allogroup (Soto and Casas, 2001), see figure 2. The carbonate slope marls of Las Paules and La Patra formations thin to the north, where they interlayer with the siliciclastic turbidites of the Hecho group represented in the east limb of the Boltaña anticline by the San Vicente Fm of Van Lunsen (1970). The Sobrarbe deltaic facies overlie La Patra Fm in the Sta. Mª Buil syncline and in the western limb of the Boltaña anticline, below the Campodarbe unconformity (transition to the Bartonian and Lower Oligocene). The Sobrarbe delta facies (De Federico, 1981; Dreyer *et al.*, 1999) are Middle to Late Lutetian in age. On the Sobrarbe delta continental siliciclastic red beds crop out in the Sta. Mª Buil syncline. They correspond to the Escanilla Fm dated as Bartonian to Lower Oligocene, based on paleomagnetic data (Bentham, 1992; Bentham and Burbank, 1996).

The studied sections correspond to the Las Paules and La Patra carbonate slope facies and the lower part of the Sobrarbe deltaic facies. These sections represent the carbonate foreland margin of the basin, whereas the Sobrarbe deltaic facies correspond to a SE to NW progradational siliciclastic wedge filling the basin trough when the deformation progresses forelandwards into the studied area (Fig. 2).

Methodology

Sampling

A water-refrigerated drill machine was used to obtain *in situ* oriented cores. Samples were taken along several profiles that may be laterally correlated, comprising a stratigraphic thickness of 900 m along the eastern limb of the Boltaña anticline (see location of profiles in figure 2). The major part of the studied sequence consists of grey marlstones and limestone marls and, more scarcely, fine grain sandstones of turbiditic origin with a Lutetian age (Mochales *et al.*, 2008). One core (two samples) was taken every 3 m of stratigraphic series. This sampling technique allows for statistical treatment of data in a continuous way, contrasting with the common grouping of samples in single sites in other AMS studies (see Filtering section below).

Measurements and parameters used

Measurements were taken with a low-susceptibility bridge, KLY-3S Kappabridge (AGICO) at the University of Zaragoza. Measurements were made at room temperature. AMS measurements give the orientations and magnitudes of the $K_{min} \leq K_{int} \leq K_{max}$ axes of the AMS ellipsoid. The primary statistical procedure was based on Jelinek's method (Jelinek, 1981). The magnetic fabric is characterised by the magnetic lineation (K_{max}) and the magnetic foliation (perpendicular to K_{min}). Scalar parameters used to characterise magnetic susceptibility are: a) the corrected anisotropy degree, *P'*, indicating the total eccentricity of the magnetic ellipsoid and thus the preferred orientation of minerals, b) *T*, the shape parameter, varying between T = -1 (prolate ellipsoids) and T = +1 (oblate ellipsoids). *P* and *T* parameters are defined as (Jelinek, 1981):

$$P' = \exp\sqrt{\{2[(\mu_1-\mu m)^2+(\mu_2-\mu m)^2+(\mu_3-\mu m)^2]\}} \quad (1),$$

$$T = \frac{(2\mu_2-\mu_1-\mu_3)}{\mu_1-\mu_3} \quad (2),$$

where $\mu_1 = \ln K_{max}$, $\mu_2 = \ln K_{int}$, $\mu_3 = \ln K_{min}$ and $\mu m = (\mu_1 + \mu_2 + \mu_3)/3$.

Furthermore, L = K1/K2 and F = K2/K3 parameters were used to define the shape of the magnetic ellipsoid as in the Flinn diagram (Flinn, 1962). Results obtained, both diagrams Flinn and *T-P'*, are shown in figure 3, thus allowing us to characterise the magnetic ellipsoids involved in this section.

Treatment of data and filtering

The sampling method used allows for a specific treatment of data that permits orientation reliable variations along the stratigraphic log to be detected. Treatment of data included the grouping of samples according to running averages of 7 samples (for the whole data), with superposition of 6 samples, in order to smooth out the orientation trend. This method allows errors deriving from different rock types to be minimised, as will be shown in the Results section.

Basic filtering of data was done according to the criteria exposed in Pueyo *et al.* (2004) using the F12, F23, F13 values by Jelinek (1981) relating eigenvectors. Clearly, oblate fabrics were not considered to calculate magnetic lineations, and strongly scattered averages (associated to pseudo-isotropic samples) were avoided by means of eigenvalues. Filtering was used in two ways, strong and soft, according to the rigidity in the application of the following exposed criteria:

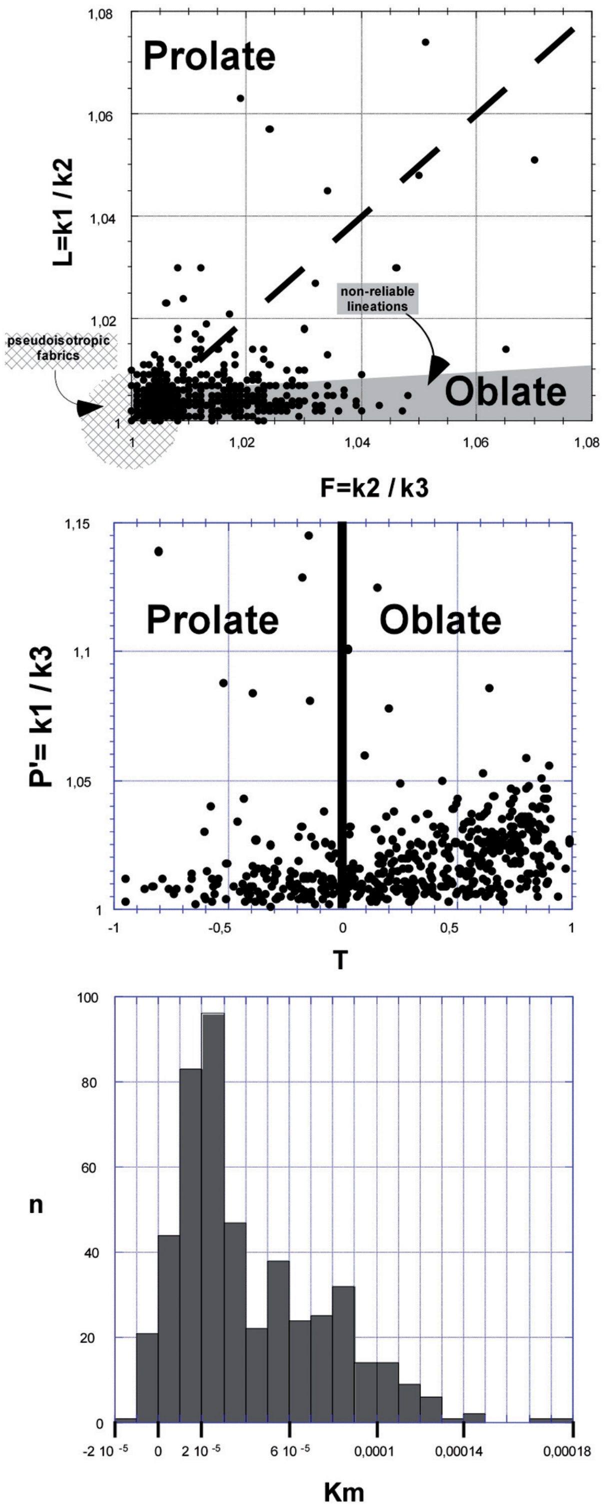

Figure 3. AMS Shape parameters expressed by means of Flinn diagram (Flinn, 1962). Magnetic fabrics show a low degree of anisotropy and are mostly oblate. Jelinek (1981) diagram also shows this tendency. The histogram indicates that the main mode of bulk susceptibility is within the paramagnetic field.

Strong filtering, consists of three sub-filterings:

1) In order to eliminate the samples that describe an isotropic magnetic ellipsoid, the parameter F13 (≈E31°) was considered. Samples with F13 < 10 were removed, so only anisotropic samples were selected.

2) With the aim of ruling out the samples with oblate magnetic ellipsoids (K1≈K2), those ellipsoids with F12 (≈E21°) < 8 were eliminated. Only samples with clearly different K1 and K2 axes were retained.

3) With the purpose of ensuring that K3 is perpendicular to bedding and K1 is contained in the bedding plane, the samples that present inclination angles lower than 60° (after bedding correction) have been removed. Only samples with K3 sub-perpendicular or perpendicular to bedding have then been considered.

In a similar way, the soft filtering consists of three sub-filtering with the same aim, but less strict application of conditions, only removing: 1) Samples with F13 < 4, 2) samples with F12 < 5, and 3) samples with K3 inclination <50°.

Results obtained after different types of filtering are shown in figures 3 and 4, thus allowing direct evaluation of the noise/signal reduction along the studied profile.

Results

Total tensor parameters

The average susceptibility of samples (Km) show intermediate values for this kind of rocks, and ranges between -12 and 184×10^{-6} (SI), the average being about 41×10^{-6} (SI). These values are within the "rock matrix" ranges (Rochette, 1987) and are typically paramagnetic as deduced from the ratios between the low field/high field susceptibilities. *P'* values are between 1.001 and 1.145, with a mean of 1.019. *T* values range from -0.951 and 0.990, with a mean of 0.2683. *L* values are between 1 and 1.112, with an average of 1.006. *F* ranges between 1 and 1.070, with a mean of 1.012.

Directional data

In general, there are no significant differences in the trend of K1 along the profile between the non-filtered and the filtered data sets, which support the consistency of the obtained results. The orientations of K1 and K3 are relatively homogeneous along the sampled profile. K3 is usually perpendicu-

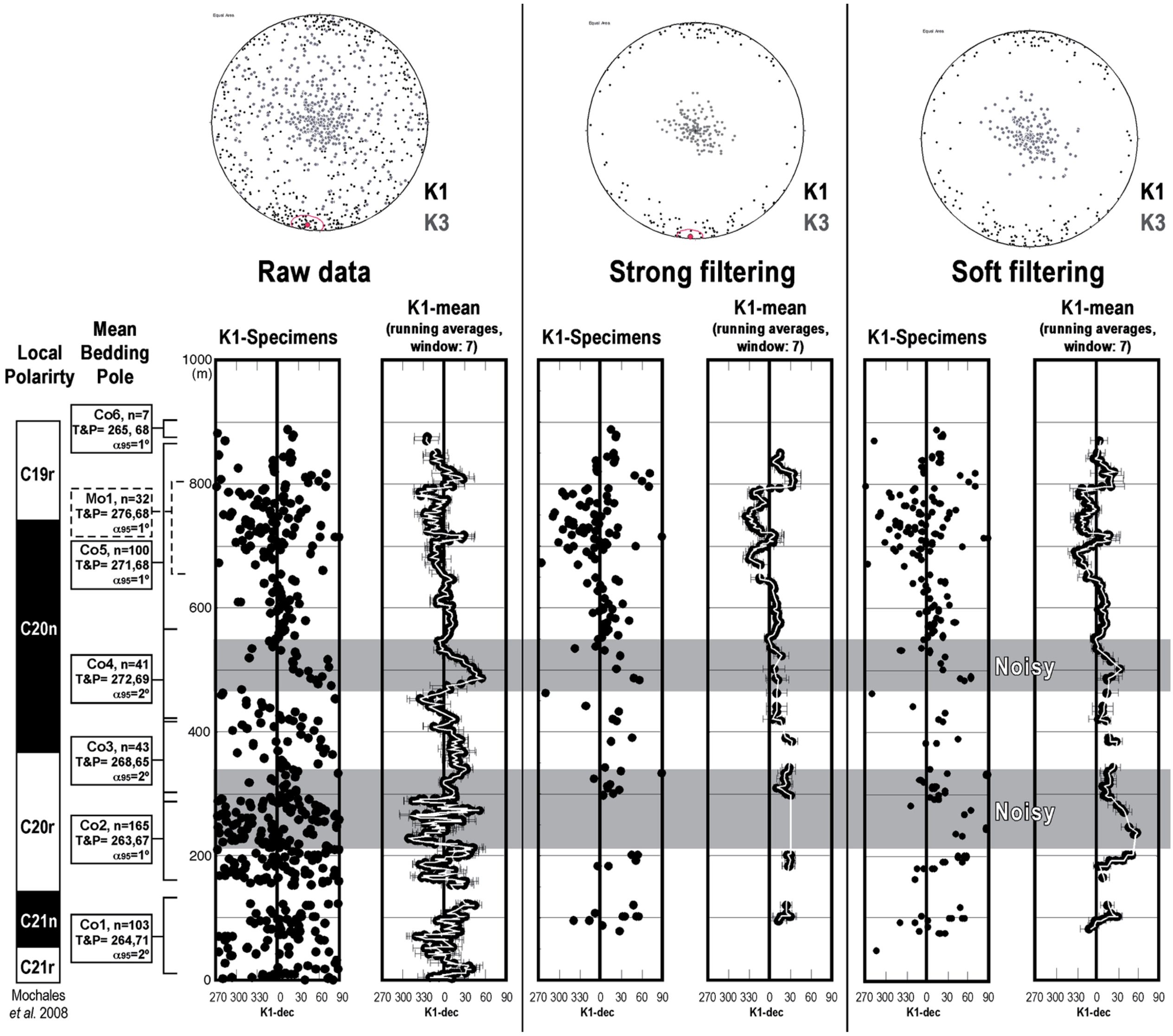

Figure 4. Stereoplots obtained from magnetic ellipsoids of the studied section, after and before filtering; K1 and K3 values are shown in black and grey, respectively. These values are situated in a stratigraphic log vs. declination of the K1 diagram. Raw data and running averages (with their standard error bar) are displayed together; grey areas present a noise signal. Subsections and the magnetostratigraphic log are shown.

lar to bedding (Fig. 5); K1 values show a clear maximum in a N-S direction, with scattering towards NNE and NNW orientations. Two other secondary maxima of K1 orientation appear in NE-SW and NW-SE directions, and can be clearly distinguished in the filtered data sets.

Considering the changes in orientation along the stratigraphic log, a slight change is observed between the lower part of the profile, where a N-S to NNE-SSW is dominant, and the upper part of the profile, with its maximum shifted toward the NNW-SSE direction (Fig. 5). However, these changes are not significant if the confidence errors are considered.

Interpretation and discussion

Directional data obtained allow an interpretation of deformation associated with the growing of the Boltaña anticline to be proposed. Relative chronology of deformation and folding evolution can be established, taking into account the tilting of fabrics (mainly obtained from the plunge of K3 axes) in the fold limbs and the clockwise rotation of the Boltaña anticline during Eocene times (Parés and Dinarès-Turrell, 1993; Pueyo, 2000; Mochales *et al.*, 2008).

An oblate sedimentary fabric would be contained in the pre-tectonic deposits. The time between the sed-

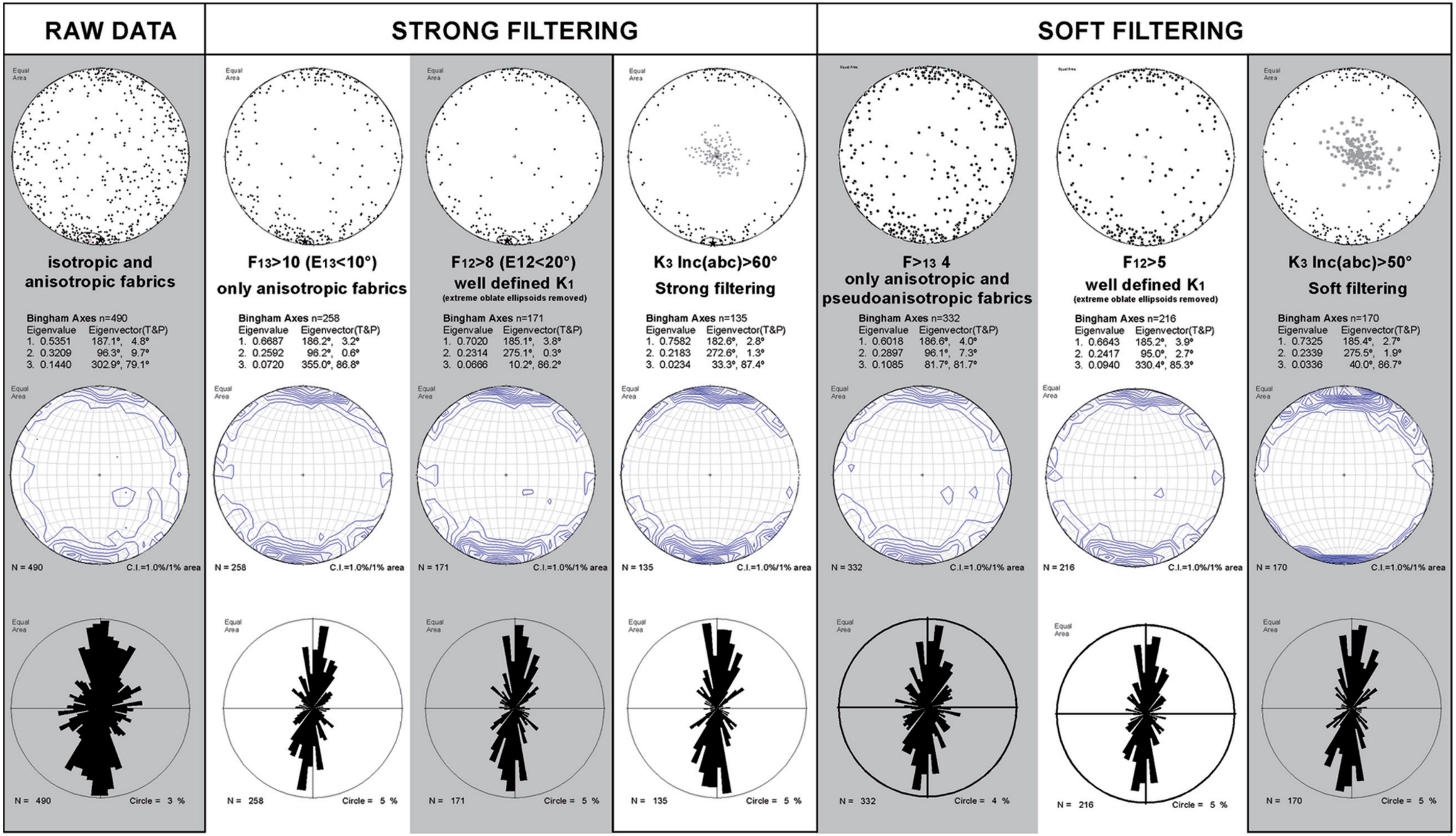

Figure 5. In columns: K1 declination from raw data and filtered data (strong and soft filtering). In rows: equal-area projection (including eigenvalues), density stereoplots and rose diagrams of K1 axes obtained through the section after step-by-step filtering.

iment deposition and blocking of the fabric ranges within a few (<10) ka after deposition (Larrasoaña *et al.*, 2004) in the Pamplona-Bartonian marls cropping out in the occidental part of the basin. Subsequently, the sediment folding reoriented the earlier fabric. Therefore, the K1 would become parallel to the main structural trend (WNW-ESE). During a final evolutionary stage, the K1 orientation changed due to fold growing as well as rotation. Currently, high K1 trend distribution appears parallel to the axis strike.

Paleomagnetic results extracted from Mochales *et al.* (2008) help us to interpret the data obtained from the AMS analysis and to propose a kinematic evolutionary model of the Boltaña anticline:

The first stage in AMS evolution in the model proposed (Fig. 6) was layer parallel shortening (LPS) in the strata that was later to be involved in the Boltaña anticline. This stage modified the earlier and oblate sedimentary fabric. The second stage was probably the growing of the Boltaña anticline, coeval with syntectonic sedimentation. Said stage resulted in the folding of the previously formed fabrics originated by LPS. The third evolutionary stage is related to the clockwise rotation of the Boltaña anticline that also rotated the magnetic ellipsoids with the same magnitude, the uplifting of the Boltaña anticline occurring at the same time. Paleomagnetic results (Mochales *et al.*, 2008) have confirmed that the third stage may be coeval, although discontinuous in time, with the deposition of the uppermost part of the stratigraphic pile. The rotation would have happened during a short space of post-Lutetian time so that all data gathered (Bentham and Burbank, 1996; Pueyo, 2000; both at higher stratigraphic locations) is meaningful. Further studies (in progress) will unravel the complete rotational kinematics of the fold. Fernández-Bellón (2004) also established three stages of deformation with rotation values progressively diminishing in younger rocks. He proposed that both stages (second and third) were simultaneous. Therefore, in this paper we consider the second and third stages as not being simultaneous. The third stage, with coeval rotation and folding, would have begun later than the age proposed by Fernández-Bellón (2004), that is, close to the Late Lutetian-Bartonian limit.

A remarkable aspect of the fabrics obtained in this work, also noted in other works on AMS in sedimentary rocks, is the existence of a single fabric (Larrasoaña *et al.*, 2003; Oliva *et al.*, 2009; Pueyo-Anchuela *et al.*, 2008), which corroborates that magnetic fabric development is a relatively early process in tectonic evolution and behaves as a passive marker of the deformation (Fig. 6).

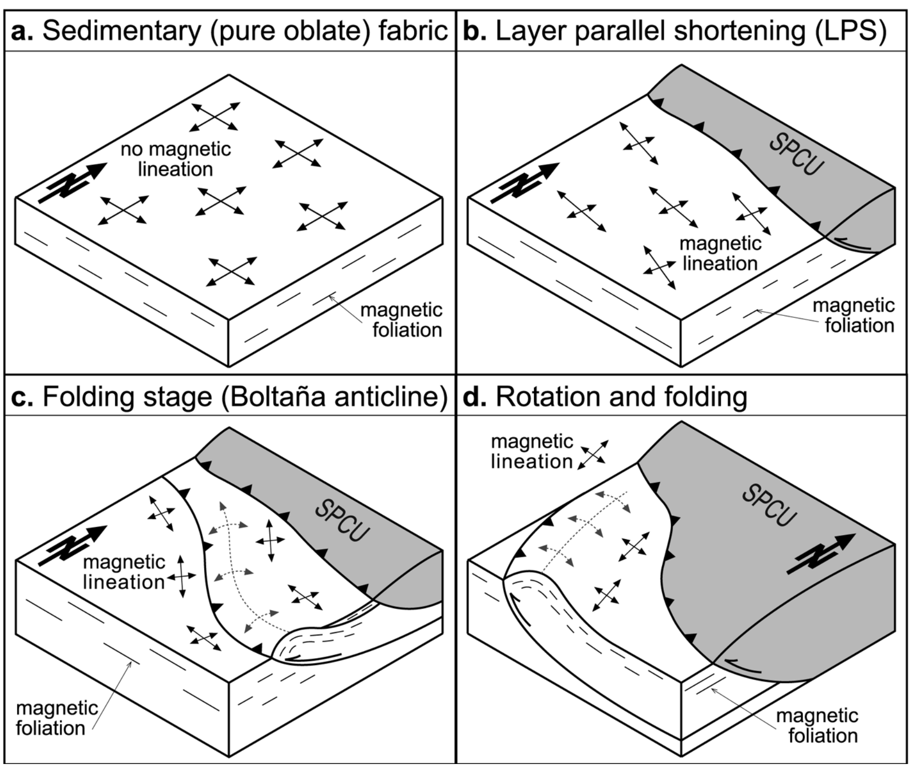

Figure 6. Model proposed to describe the role of AMS during the formation of Boltaña anticline. Sedimentary fabric (a) is modified by LPS (b) and later folded by the Boltaña anticline (c). During the emplacement of the SPCU, the structure rotated as a whole, adopting a N-S trend (d). Therefore, AMS behaved as a passive marker.

Acknowledgements

Research financial support comes from the projects Pmag3Drest (CGL-2006-2289-BTE MEC and CGL2009-14214 MICINN), 3DR3 & GeoPyrDatabases (PI165/09 and CTPP01/07 Gob. Aragón) and AMS (CGL2006-05817/BTE and CGL2009-08969) and a pre-doctoral grant from the Instituto Geológico y Minero de España awarded to Tania Mochales. The authors are grateful to Sylvia Gracia for support in laboratory analysis of AMS samples and Josep Poblet for the revision of this manuscript.

References

Barnolas, A., Samsó, J. M., Teixell, A., Tosquella, J. and Zamorano, M. (1991): Evolución sedimentaria entre la cuenca de Graus-Tremp y la cuenca de Jaca-Pamplona. *I Congreso del Grupo Español del Terciario. Libro-Guía de la excursión nº 1, EUMO* Gràfic, Vic, 123 pp.

Bentham, P. (1992): *The tectono-stratigraphic development of the western oblique ramp of the south-central Pyrenean thrust system, Northern Spain*. PhD Thesis, University of Southern California, 253 pp.

Bentham, P. and Burbank, D. W. (1996): Chronology of Eocene foreland basin evolution along the western oblique margin of the South-Central Pyrenees. In: C. Dabrio and P. Friend (eds): *Tertiary basins of Spai*n: 144-152.

Cámara, P. and Klimowitz, J. (1985): Interpretación geodinámica de la vertiente centro-occidental surpirenaica (Cuencas de Jaca-Tremp). *Est. Geol.*, 41: 391-404.

De Federico, A. (1981): La sedimentación de talud en el sector occidental de la cuenca paleógena de Ainsa, *Publ. Geología,* Universidad Autónoma de Barcelona, 12: 271 pp.

Dreyer, T., Corregidor, J., Arbués, P. and Puigdefábregas, C. (1999): Architecture of the tectonically influenced Sobrarbe deltaic complex in the Ainsa Basin, northern Spain. *Sediment. Geol.*, 127: 127-169.

Fernández Bellón, O. (2004): *Reconstruction of geological structures in 3D: an example from the Southern Pyrenees*. PhD Thesis, Universitat de Barcelona, 321 pp.

Flinn, D. (1962): On folding during three-dimensional progressive deformation. *Geol. Soc. London Q. J.*, 118: 385-433.

Jelinek, V. (1981): Characterization of the magnetic fabric of rocks. *Tectonophysics*, 79: T63-T67.

Larrasoaña, J. C., Parés, J. M., Millán, H., del Valle, J. and Pueyo, E. L. (2003): Paleomagnetic, structural and stratigraphic constraints on transverse fault kinematics during basin inversion: the Pamplona Fault (Pyrenees, N Spain). *Tectonics*, 22: doi:10.1029/2002/TC001446.

Larrasoaña, J. C., Pueyo, E. L. and Parés, J. M. (2004): An integrated AMS, structural, palaeo- and rock-magnetic study of the Eocene marine marls from the Jaca-Pamplona basin (Pyrenees, N Spain); new insights into the timing of magnetic fabric acquisition in weakly deformed mudrocks. In: F. Martín-Hernández, C. M. Lüneburg, C. Aubourg and M. Jackson (eds): *Magnetic fabric: methods and applications*, *M. Geol. Soc. London Spec. Publ.*, 238: 127-144.

Martín-Hernández, F. and Hirt, A. M. (2003): The anisotropy of magnetic susceptibility in biotite, muscovite and chlorite single crystals. *Tectonophysics*, 367: 13-28.

Mochales, T, Pueyo E. L., Casas, A. M. and Barnolas, A. (2008): Cinemática rotacional del anticlinal de Boltaña (Pirineo Occidental) durante el Luteciense. *Geotemas*, 10: 1179-1182.

Oliva, B., Pueyo, E. L., Larrasoaña, J. C., Gil-Imaz, A., Mata, P., Parés, J. M. and Schleicher, A. M. (2009): Complex magnetic subfabrics in a well-developed cleavage domain, Internal Sierras (Pyrenees, Spain). *J. Struct. Geol.*, 31: 163-176. doi:10.1016/j.jsg.2008.11.002

Parés, J. M., Van der Pluijm, B. A. and Dinarès-Turell, J. (1999): Evolution of magnetic fabrics during incipient deformation of mudrocks (Pyrenees, northern Spain). *Tectonophysics*, 307: 1-14

Parés, J. M. and Dinarès-Turrell, J. (1993): Magnetic fabric in two sedimentary rock types from the South Pyrenees. *J. Geomagn. Geoelectr.*, 45: 193-205.

Pueyo, E. L., Millán, H., Pocoví, A. and Parés, J. M. (1999): Cinemática rotacional del cabalgamiento basal surpirenaico en las Sierras Exteriores Aragonesas: datos magnetotectónicos. *Acta Geol. Hisp.*, 32, 3-4: 237-256.

Pueyo, E. L. (2000): *Rotaciones paleomagnéticas en sistemas de cabalgamientos; Tipos, causas, significado y aplicaciones (Ejemplos de las Sierras Exteriores y de la Cuenca de Jaca, Pirineo Aragonés)*. PhD Thesis, Universidad Zaragoza, 299 pp.

Pueyo, E. L., Román, M. T, Bouchez, Casas, A. M. and Larrasoaña, J. C. (2004): Statistical significance of magnetic fabric data in studies of paramagnetic granites. In: F. Martín-Hernández, C. M. Lüneburg, C. Aubourg and M. Jackson (eds): *Magnetic fabric: methods and applications*, *M. Geol. Soc. London Spec. Publ.*, 238: 395-420.

Pueyo-Anchuela, O., Gil-Imaz, A., Pocoví, A. and Pueyo E. L. (2008): AMS as a fast and sensitive method to test and detect vertical axis rotation in fold and thrust systems. Southern Pyrenees, Aragón, Spain. *Geophys. Res. Abstr.*, 10: EGU2008-A-07853.

Puigdefábregas, C. (1975): La sedimentación molásica en la cuenca de Jaca. *Pirineos*, 104: 1-188.

Rochette, P. (1987): Magnetic susceptibility of the rock matrix related to magnetic fabric studies. *J. Struct. Geol.*, 9: 1015-1020.

Soto, R. and Casas, A. M. (2001): Geometría y cinemática de las estructuras norte-sur de la cuenca de Ainsa. *Rev. Soc. Geol. España*, 14: 3-4.

Soto, R., Mattei, M. and Casas, A. M. (2003): Relationship between AMS and folding in an area of superimposed folding (Cotiella-Bóixols nappe, Southern Pyrenees). *Geodin. Acta*, 16: 171-185.

Soto, R., Casas-Sainz, A. M., Villalaín, J. J. and Oliva-Urcía, B. (2007): Mesozoic extension in the Basque-Cantabrian Basin (N Spain): Contributions from AMS and brittle mesoestructres. *Tectonophysics*, 445: 373-394.

Van Lunsen, H. (1970): Geology of the Ara-Cinca region, Spanish Pyrenees. Province of Huesca. *Geol. Ultraiectina*, 16: 1-119.